

## Supporting Information for

### Accelerated Hydrolytic Degradation of Ester-Containing Biobased Epoxy Resins

*Minjie Shen,<sup>a</sup> Rawan Almallahi,<sup>a</sup> Zeshan Rizvi,<sup>a,b</sup> Eliud Gonzalez-Martinez,<sup>a,b</sup> Guozhen Yang,<sup>a</sup>  
and Megan L. Robertson<sup>ac\*</sup>*

<sup>a</sup> Department of Chemical and Biomolecular Engineering, University of Houston,  
4726 Calhoun Road, Houston, TX 77204-4004, United States

<sup>b</sup> Houston Community College, Houston, TX 77082, United States

<sup>c</sup> Department of Chemistry, University of Houston, Houston, TX 77204-4004, United States

\*Corresponding author  
Megan Robertson  
4726 Calhoun Road  
S222 Engineering Building 1  
University of Houston  
Houston, TX 77204-4004  
[mrobertson@uh.edu](mailto:mrobertson@uh.edu)  
713-743-2748

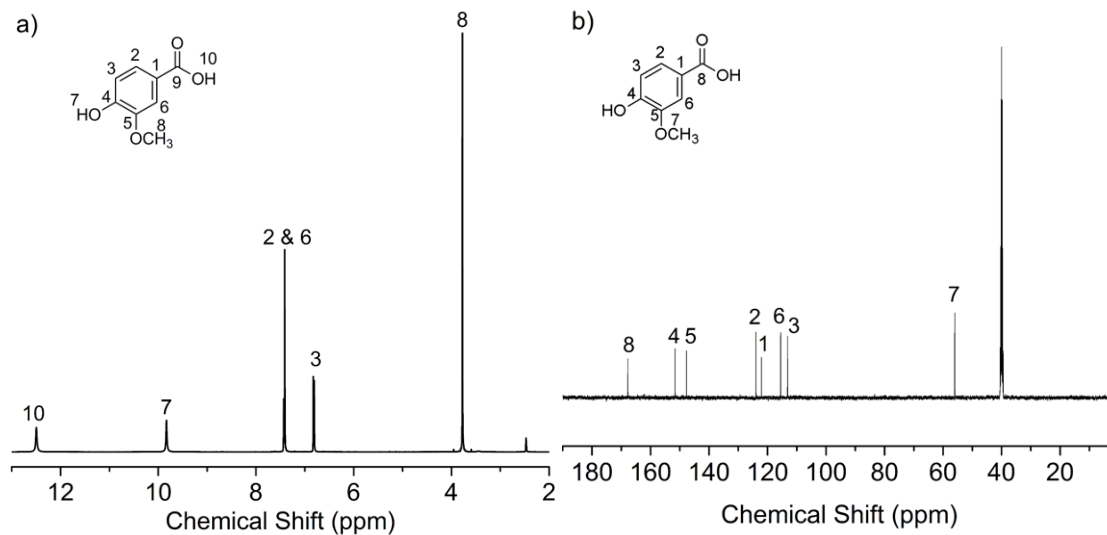


**Figure S1:** a)  $^1\text{H}$  NMR and b)  $^{13}\text{C}$  NMR data obtained from VA.

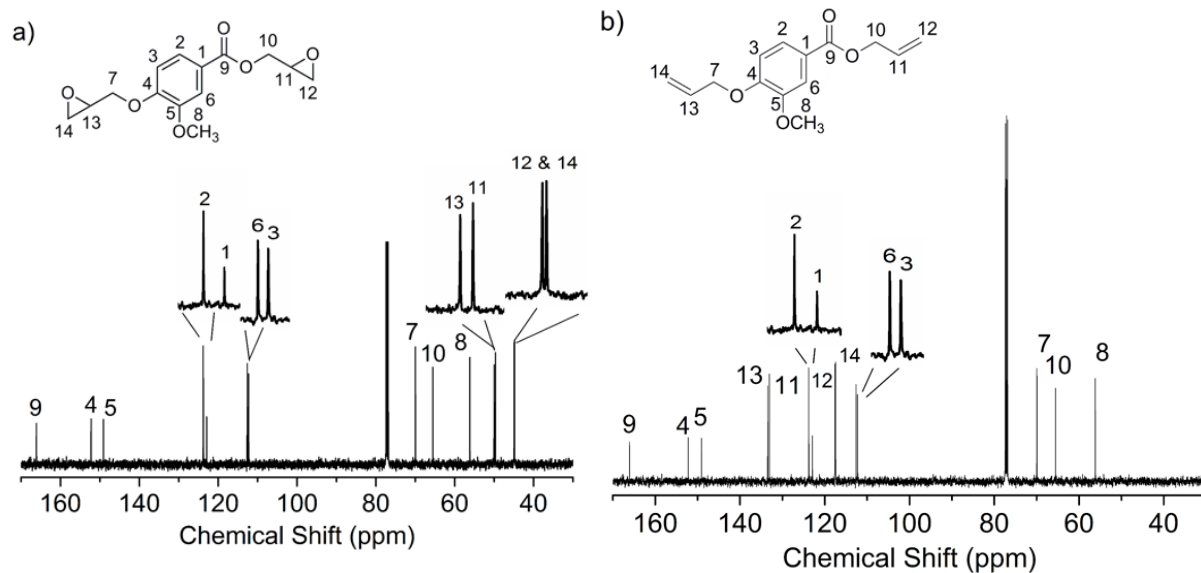
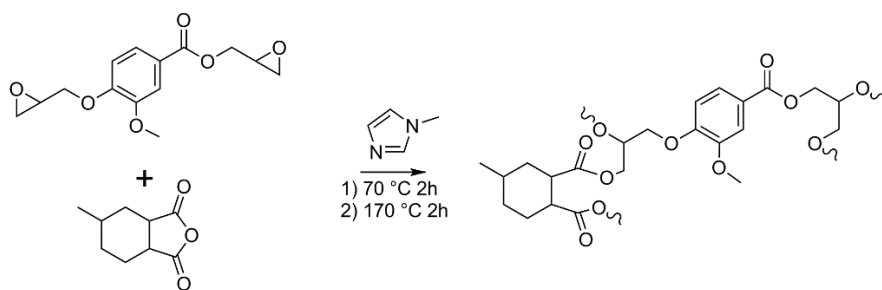
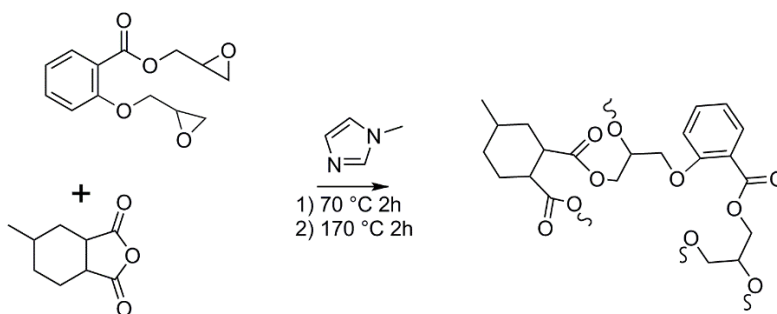


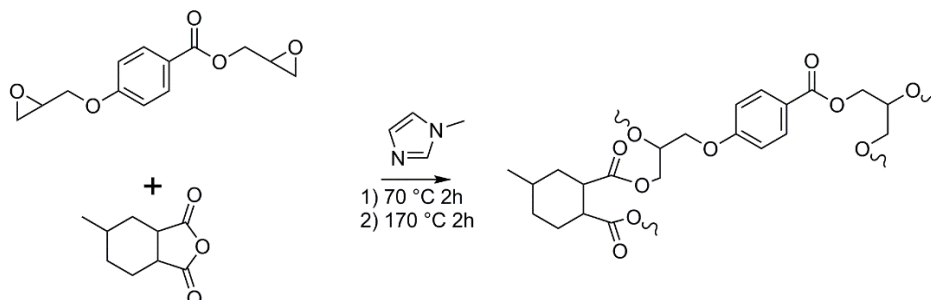
**Figure S2:**  $^{13}\text{C}$  NMR data obtained from a) EVA and b) AVA.



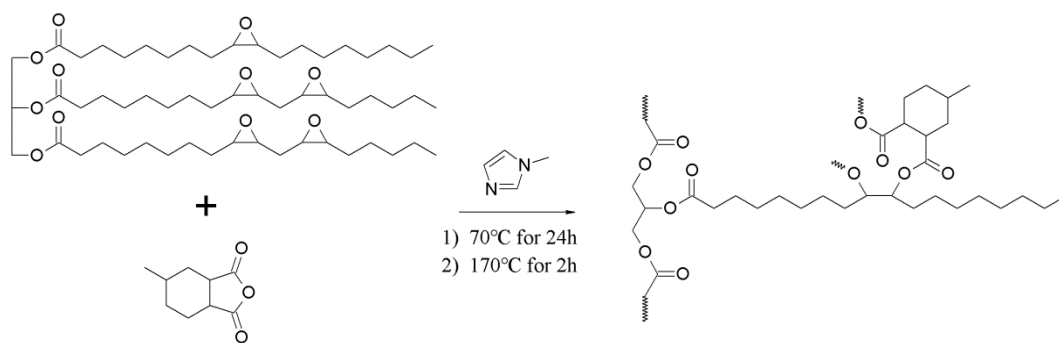
**Scheme S1:** Curing of EVA with MHPHA (catalyzed by 1-MI) to form an epoxy resin.



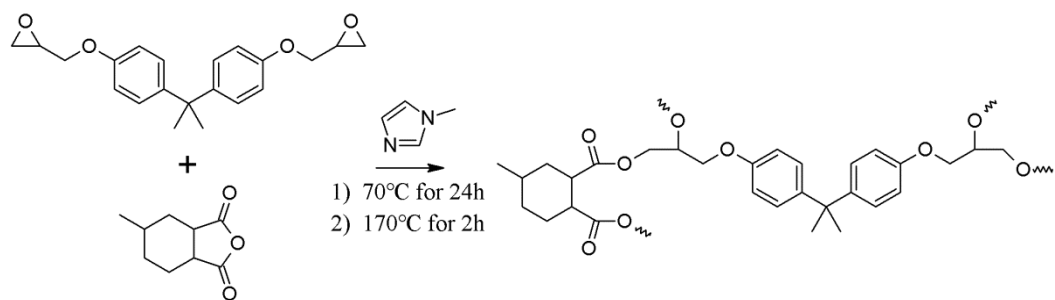
**Scheme S2:** Curing of ESA with MHPHA (catalyzed by 1-MI) to form an epoxy resin.



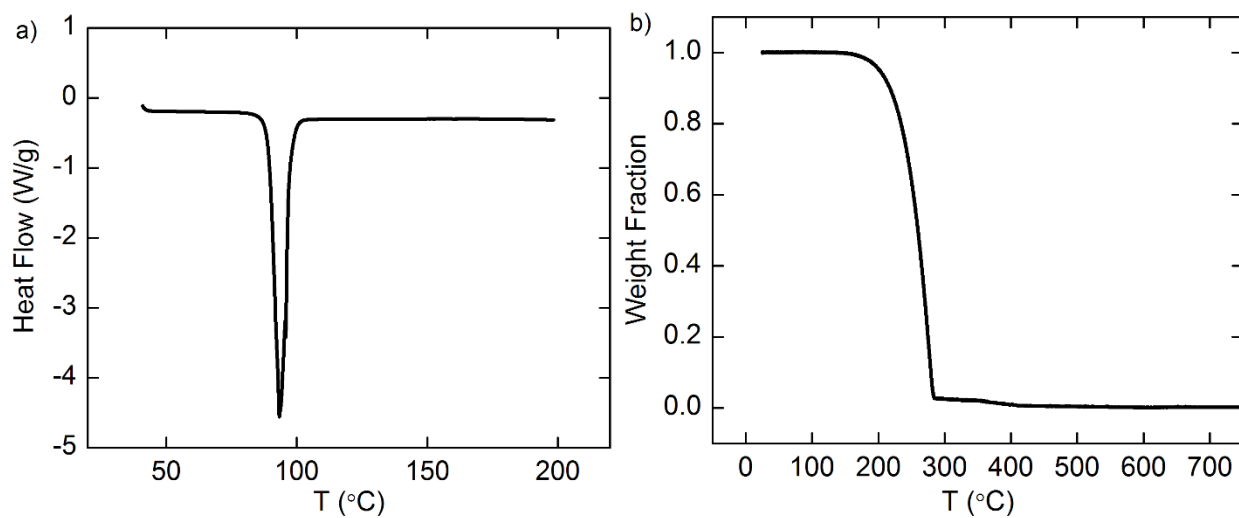
**Scheme S3:** Curing of E4HBA with MHPHA (catalyzed by 1-MI) to form an epoxy resin.



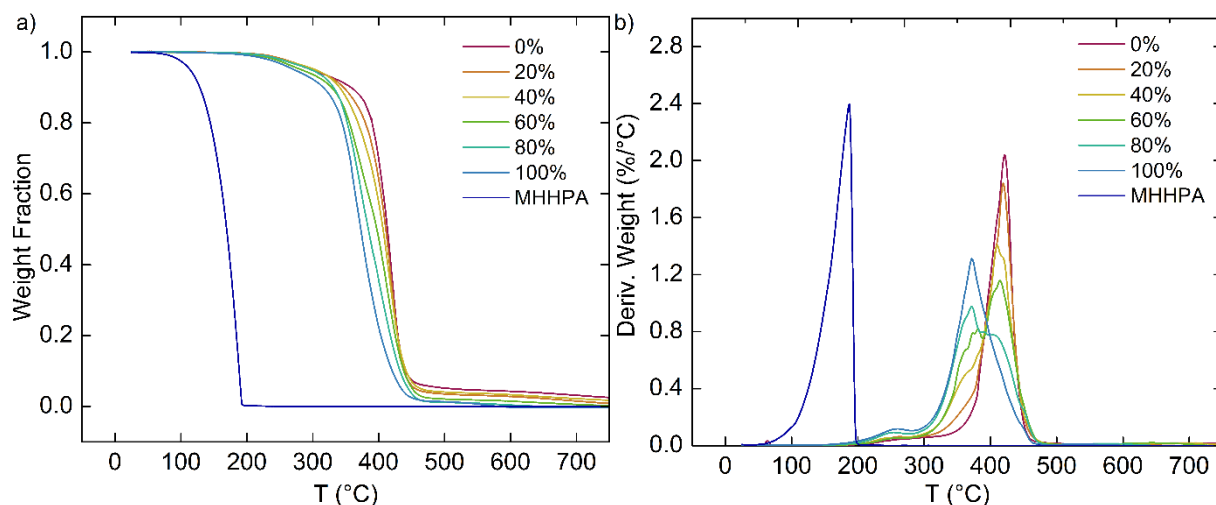
**Scheme S4:** Curing of ESO with MHPHA (catalyzed by 1-MI) to form an epoxy resin.



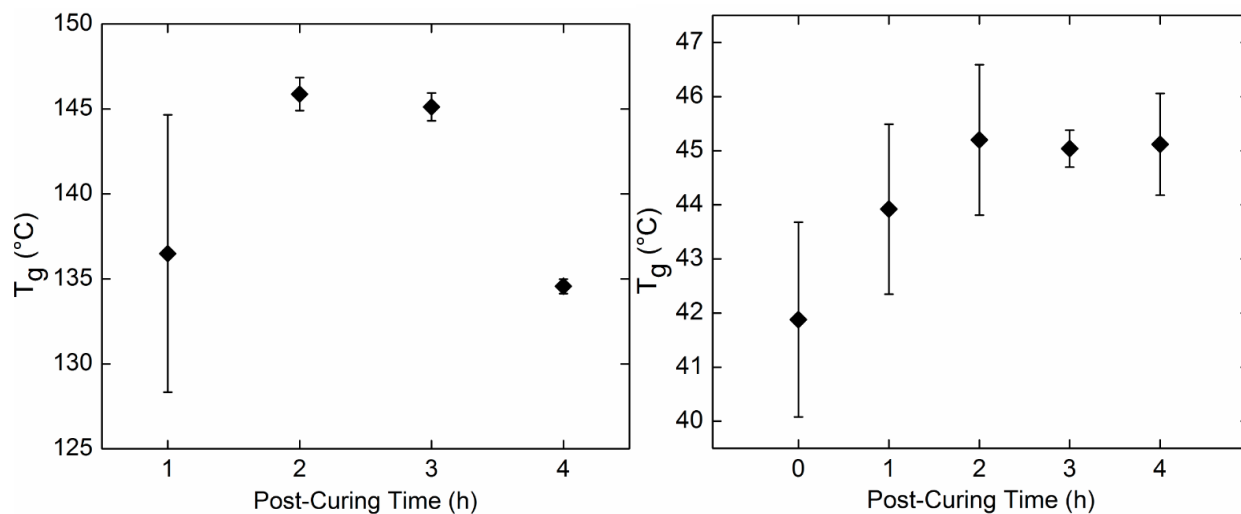
**Scheme S5:** Curing of DGEBA with MHHPA (catalyzed by 1-MI) to form an epoxy resin.



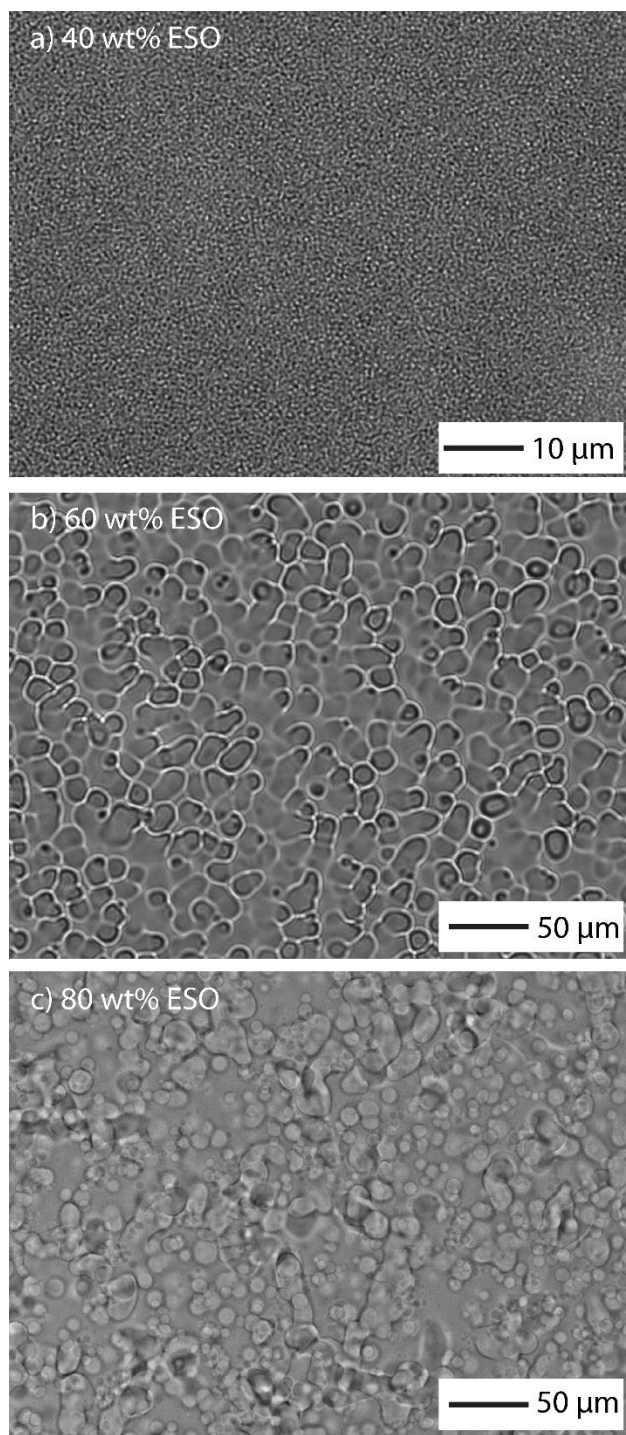
**Figure S3:** a) DSC data and b) TGA data obtained from the EVA monomer.



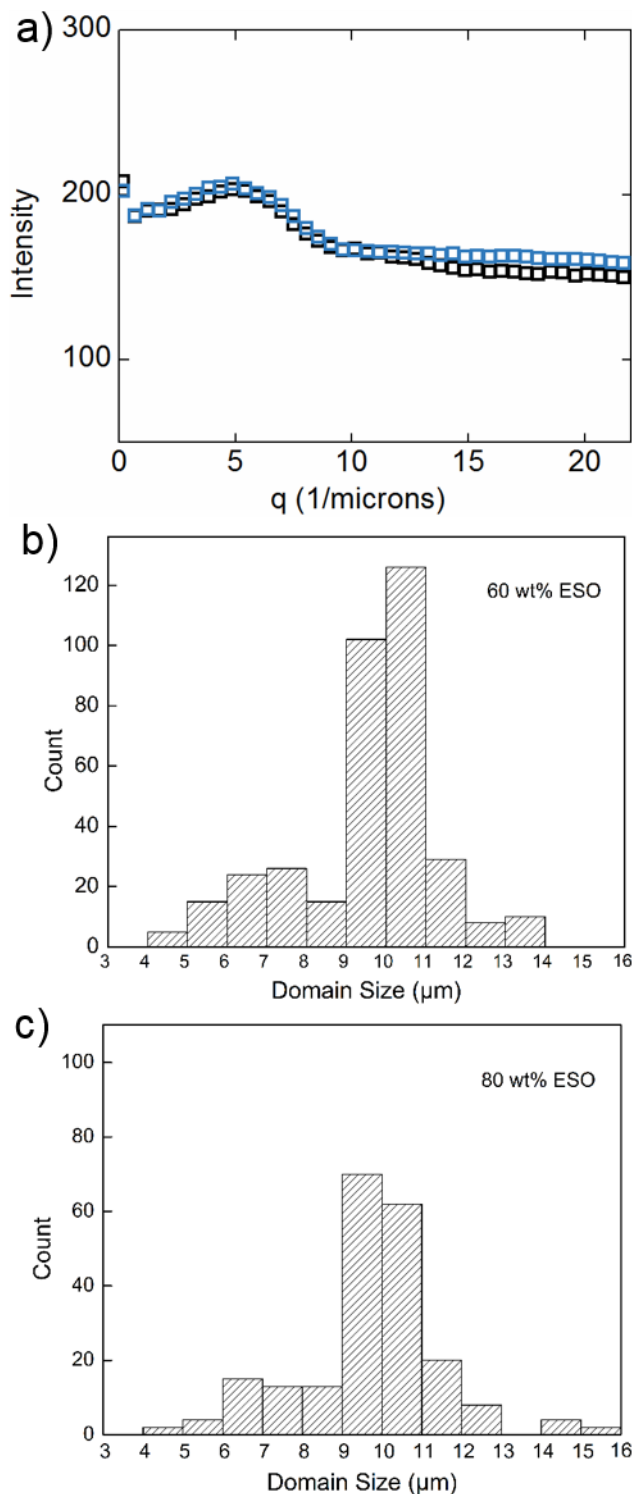
**Figure S4:** Weight loss and derivative weight loss as functions of temperature, from TGA, for epoxy resins containing different ESO and DGEBA contents (% ESO is the % relative to total amount of ESO and DGEBA). MHHPA curing agent is included for comparison purposes.



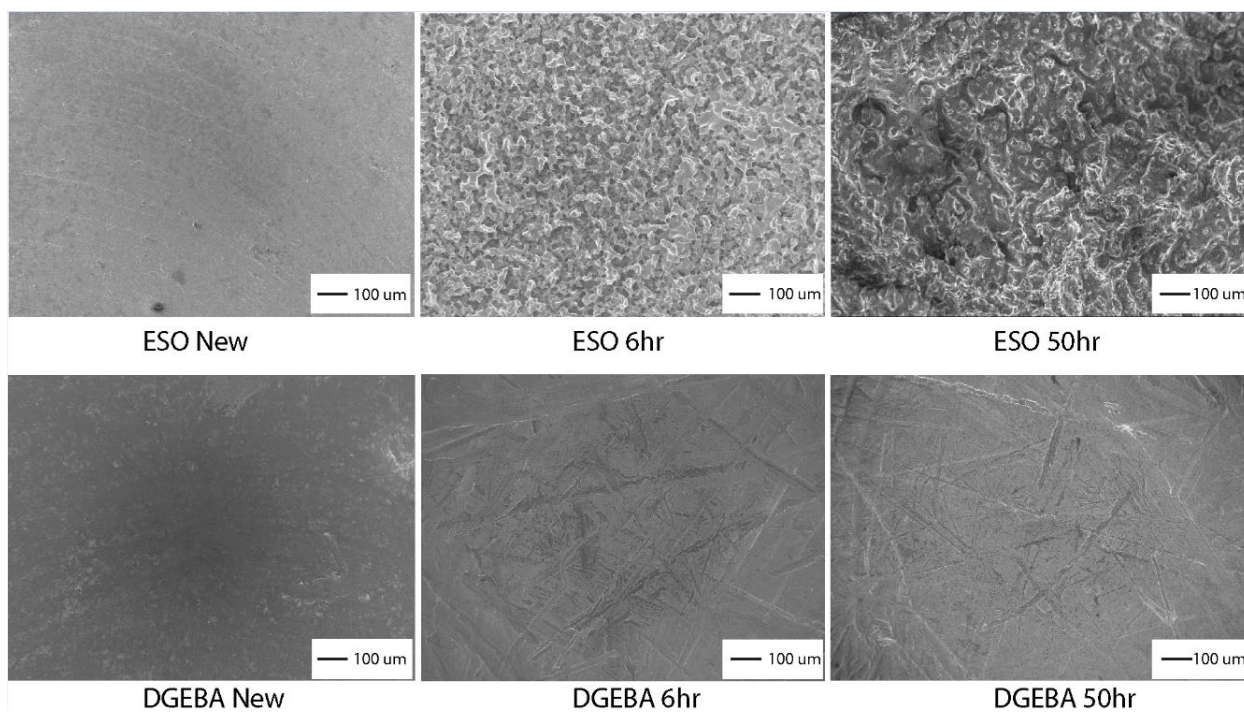
**Figure S5:** Glass transition temperature ( $T_g$ ) as a function of post-curing time at 170 °C for a) EVA- and b) ESO-based epoxy resins. Epoxy monomers were cured with MHHPA (catalyzed by 1-MI) through a two-stage process: stage 1 at 70 °C (2 h for EVA and 24 h for ESO), followed by stage 2 at 170 °C (for the time indicated on the plots). Error bars indicate repeat measurements on multiple specimens.



**Figure S6:** Optical microscopy images of epoxy resins after first-stage curing with differing ESO content (wt% ESO is the ESO content relative to the total amount of ESO and DGEBA).



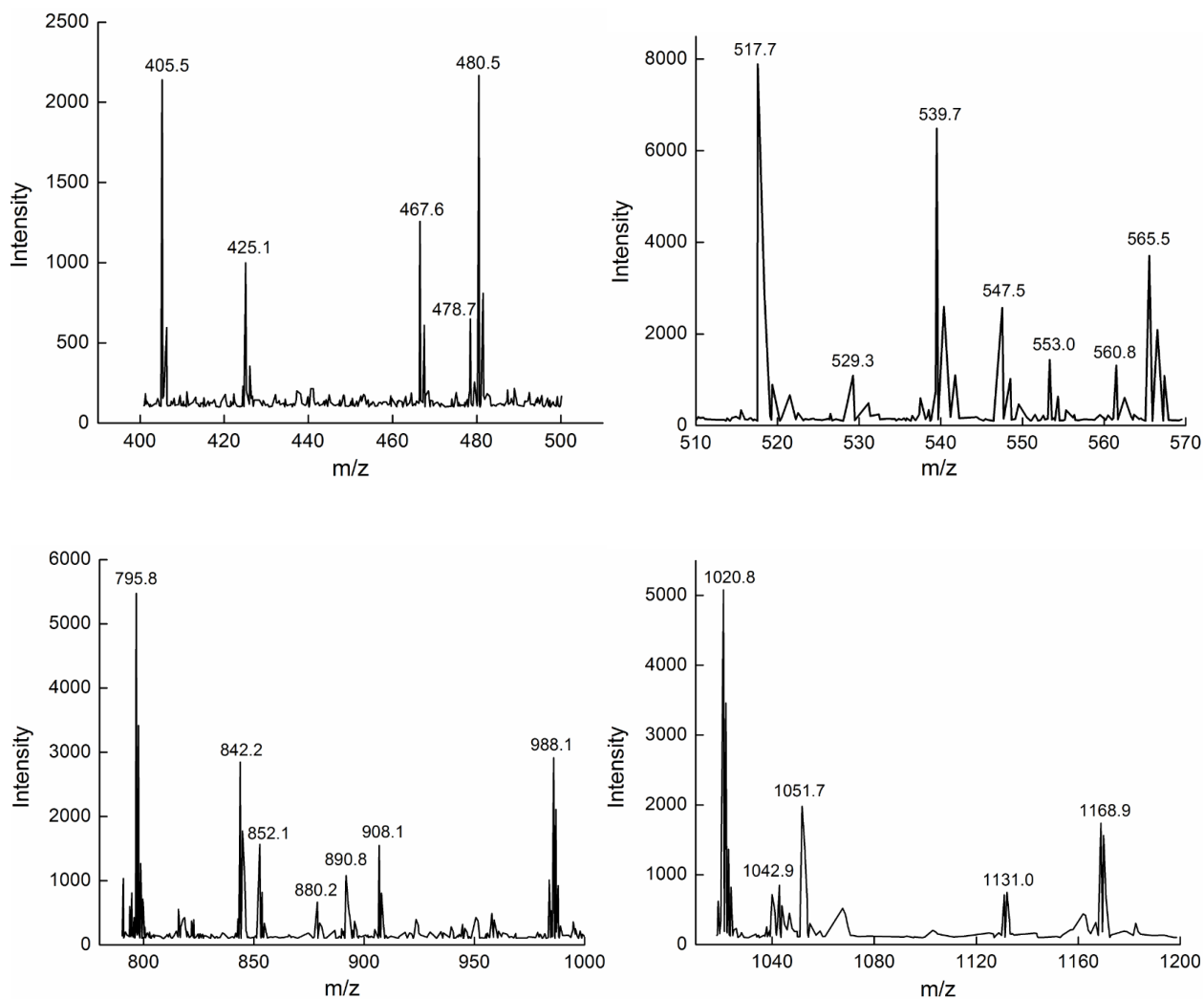
**Figure S7:** a) Intensity vs.  $q$ , obtained through the fast Fourier transform (FFT) of optical micrographs obtained from an epoxy resin containing 40 wt% ESO (of the total ESO and DGEBA monomer), prior to curing (black squares) and following curing with MHHPA/1-MI (blue squares). b, c) Particle size distributions obtained through image analysis of optical micrographs showing in Figure 5 in the main text (obtained following second stage of curing).



**Figure S8:** SEM images of the surfaces of ESO-based and DGEBA-based epoxy resins, showing surface changes after soaking in a 3wt% NaOH solution at 80 °C for 6 and 50 h.

### Analysis of mass spectrometry data obtained from ESO-based epoxy resin degradation products

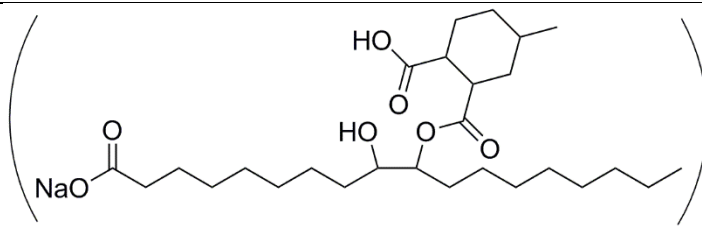
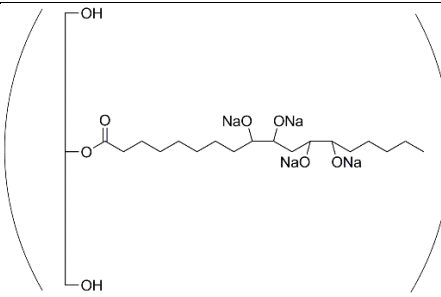
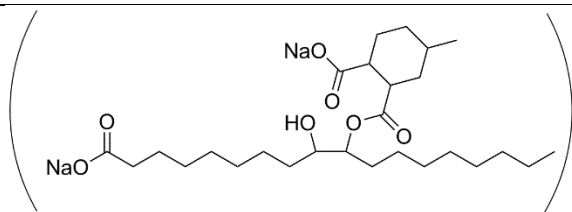
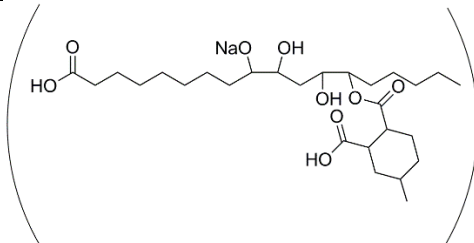
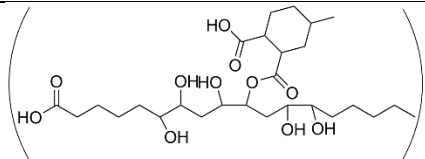
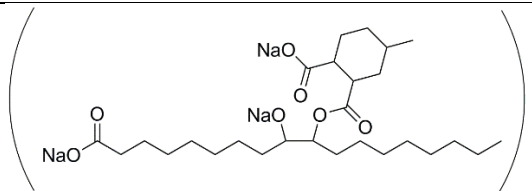
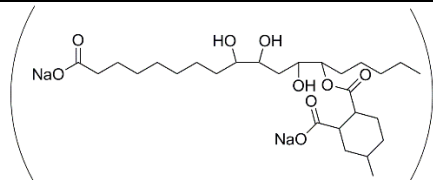
We assume the epoxy resin degradation proceeds through cleavage of ester groups. The ESO monomer contains ester groups, and the curing reaction between MHPA and ESO also produces ester groups. Esters groups are therefore dispersed throughout the epoxy network. We considered all possible combinations of fatty acids on the soybean oil triglyceride, and we also considered the presence of either  $H^+$  or  $Na^+$  ions, and the possibility of exchange between H and Na within the molecules. We then assigned the observed mass spectrometry peaks to theoretical epoxy network fragments post-degradation, as outlined below.



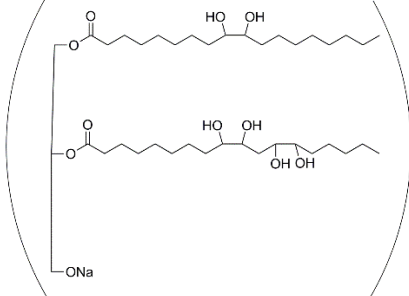
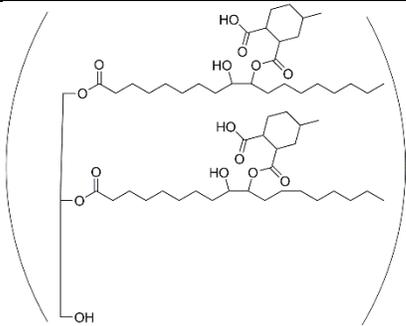
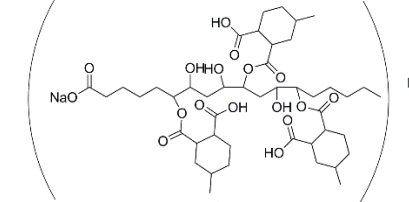
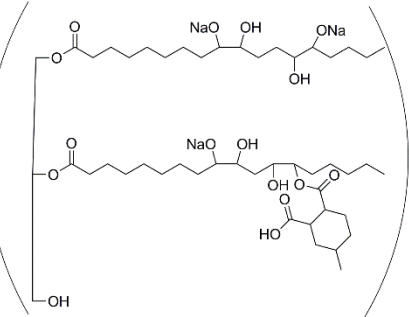
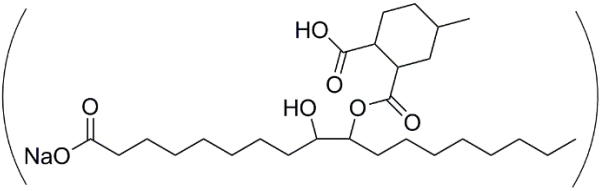
**Figure S9:** Closer view of mass spectra obtained from degradation products of an ESO-based epoxy resin.

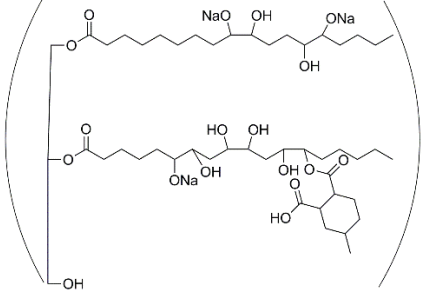
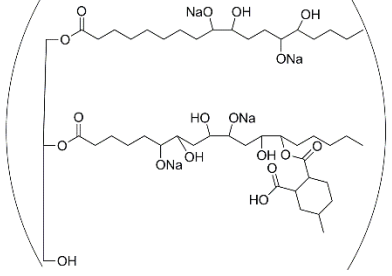
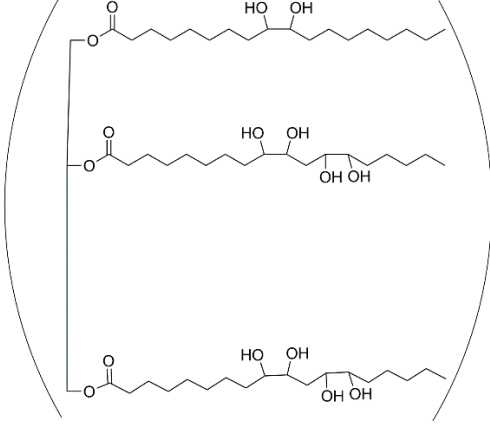
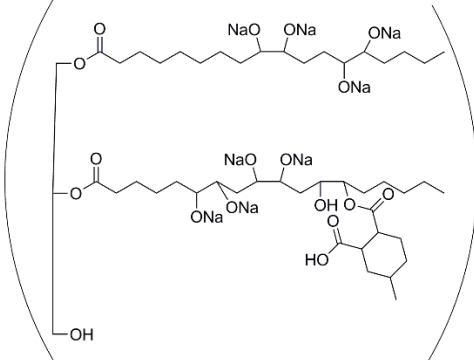
**Table S1:** Proposed chemical structures and theoretical molecular weights for peaks detected in mass spectrum (major peaks indicated in red, also discussed in main text).

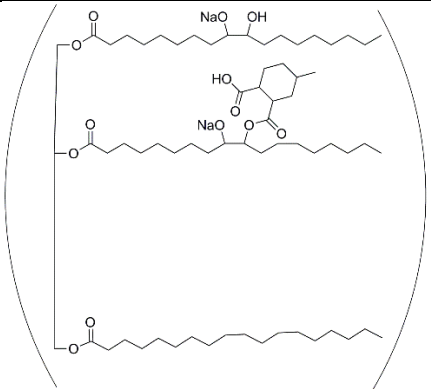
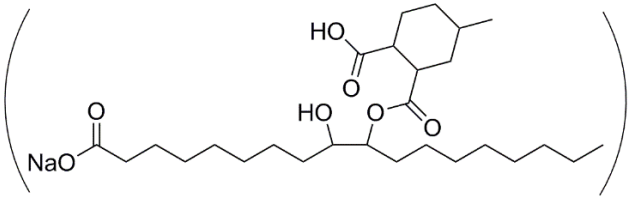
Code	Chemical Structure	Theoretical Molecular Weight (g/mol)	Observed m/z (g/mol)
1		405.4	405.5
2		425.5	425.1
3		467.5	467.6
4		477.8	478.7
5		481.3	480.5

6		H <sup>+</sup>	506.6	506.5
7		H <sup>+</sup>	517.5	517.7
8		H <sup>+</sup>	529.8	529.3
9		H <sup>+</sup>	539.7	539.7
10		H <sup>+</sup>	546.9	547.5
11		H <sup>+</sup>	553.2	553.0
12		H <sup>+</sup>	560.7	560.8

13		565.7	565.5
<b>14</b>		<b>788.0</b>	<b>787.8</b>
15		795.9	795.8
16		841.9	842.2
17		851.6	852.1

18		880.6	880.2
19		890.5	890.8
20		907.9	908.1
21		988.3	988.1
<b>22</b>	 <p>Two-molecule aggregate of structure 6</p>	<b>1012.0</b>	<b>1011.9</b>

23		1020.2	1020.8
24		1042.2	1042.9
25		1052.5	1051.7
26		1130.2	1131.0

27		1168.7	1168.9
28	 <p data-bbox="430 808 941 850">Three-molecule aggregate of structure 6</p>	1517.5	1517.5

## Solid-State Kinetic Models

The general formula for solid-state, heterogeneous kinetics is<sup>1-3</sup>

$$\frac{d\alpha}{dt} = kf(\alpha)$$

Many models have been proposed based on mechanistic assumptions, including nucleation, diffusion, geometrical contraction, and reaction-order models. The choice of a model for solid-state kinetics is based on statistical fits of mathematical models to data, supported by complementary measurements such as scanning electron microscopy, mass spectrometry, etc.

Reaction-order models involve the reaction order in the rate law, and are similar to the rate expressions in homogenous kinetics. We considered first and second-order reaction models.

Diffusion models assumes the rate-limiting step is the diffusion of reactants into reaction sites or products leaving reaction sites.

Geometrical contraction models assume the rate limiting step is the progress of the product layer from the surface to the interior of the specimen, which is related to the sample morphology. We extended the contracting volume model from a cubic specimen, as previously described,<sup>2</sup> to a cuboid specimen (i.e., side lengths a, b and c are not equal). The derivation of the model is shown in the next section.

Nucleation models assume the rate-limiting step is the formation and growth of nuclei. However, based on the shape of the curve of the mass fraction remaining versus time, nucleation models were not suitable choices for our degradation data. We therefore did not investigate these further in this study.

All the general formulae of the models are listed as below. We chose to use degradation data obtained from the ESA-based epoxy resin and DGEBA/ESO-based epoxy resin (with 40% ESO) as model samples for probing the best choice of model to fit the data.

Nucleation model:  $f(\alpha) = \alpha(1 - \alpha)$  (S1)

3D diffusion model:  $f(\alpha) = \frac{3(1 - \alpha)^{2/3}}{2(1 - (1 - \alpha)^{1/3})}$  (S2)

Contracting volume model:  $f(\alpha) = 3(1 - \alpha)^{2/3}$  (S3)

First-order reaction model:  $f(\alpha) = (1 - \alpha)$  (S4)

Second-reaction model:  $f(\alpha) = (1 - \alpha)^2$  (S5)

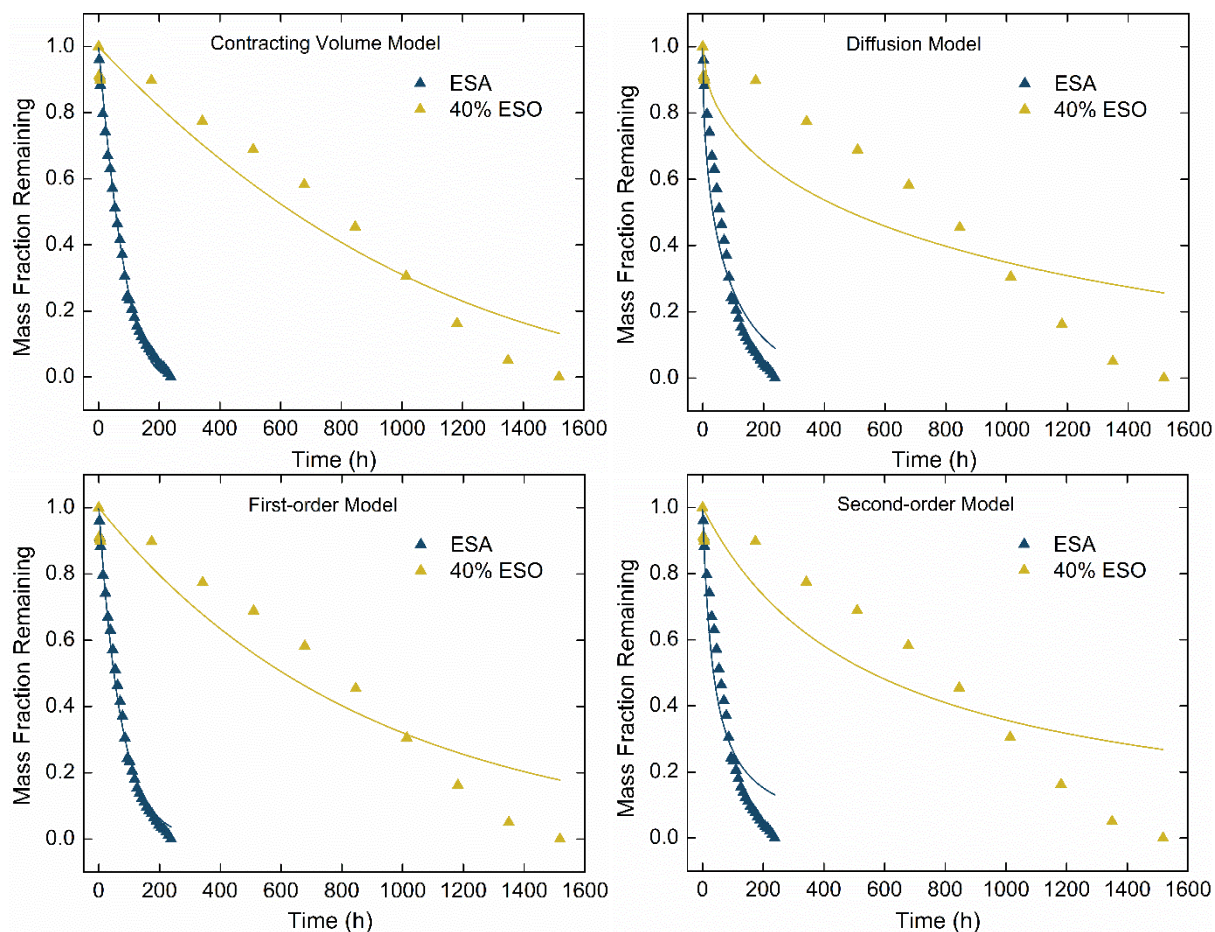


**Figure S10:** Solid-state kinetic models fit to degradation data obtained from ESA and ESO/DGEBA (40% ESO)-based epoxy resins.

**Table S2:**  $R^2$  values obtained during the fit of various solid-state kinetic models to degradation data obtained from epoxy resins.

	ESA	ESO/DGEBA (40% ESO)
Contracting Volume Model	0.997	0.958
First-order Model	0.984	0.905
Second-order Model	0.961	0.883
Diffusion Model	0.928	0.800

Contracting volume model, as applied to a cuboid sample with side lengths a, b and c (a ≠ b ≠ c)

For solid-state kinetic analysis, the conversion fraction ( $\alpha$ ) can be defined as:

$$\alpha = \frac{m_0 - m_t}{m_0} = 1 - \frac{m_t}{m_0} \quad (\text{S6})$$

where  $m_0$  is the initial weight and  $m_t$  is the weight when time =  $t$ .

For a cuboid rectangular sample (side lengths of a, b, c), and assuming 1)  $k$  doesn't change over time and 2) the cuboid retains its aspect ratio while undergoing contraction, then

$$a_0 - a = kt \quad (\text{S7})$$

$$b_0 - b = \frac{b_0}{a_0} kt \quad (\text{S8})$$

$$c_0 - c = \frac{c_0}{a_0} kt \quad (\text{S9})$$

where  $a_0, b_0, c_0$  are the initial lengths of the cuboid rectangular sample,  $a, b, c$  are the lengths of the cuboid rectangular sample at time =  $t$ ,

Using the relationship between density and mass, S6 becomes:

$$\alpha = 1 - \frac{\rho abc}{\rho a_0 b_0 c_0} = 1 - \frac{abc}{a_0 b_0 c_0} \quad (\text{S10})$$

Then, substituting S10 into S7-S9:

$$\alpha = 1 - \frac{a^3 \frac{b_0 c_0}{a_0^2}}{a_0 b_0 c_0} = 1 - \frac{a^3}{a_0^3} \quad (\text{S11})$$

$$1 - \alpha = \left( \frac{a_0 - kt}{a_0} \right)^3 = \left( 1 - \frac{kt}{a_0} \right)^3 \quad (\text{S12})$$

$$1 - (1 - \alpha)^{\frac{1}{3}} = \frac{kt}{a_0} \quad (\text{S13})$$

A new rate constant is defined as  $k/a_0$ :

$$1 - (1 - \alpha)^{\frac{1}{3}} = k't \quad (\text{S14})$$

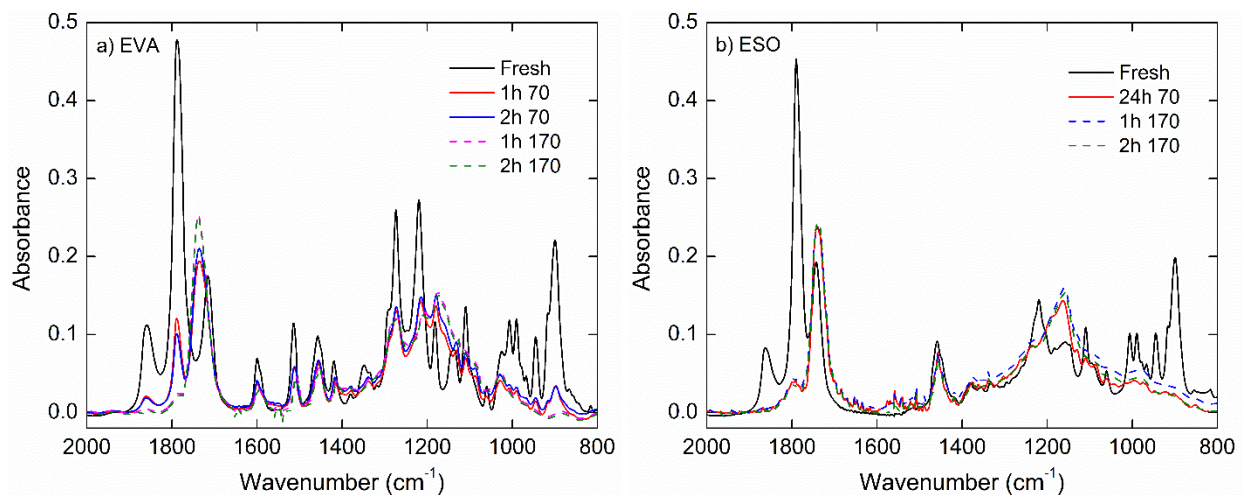


**Figure S11:** FTIR data obtained during the curing of EVA and ESO.

**Table S3:** Conversion of Epoxy Resins Quantified through FTIR

Curing Time (h) at 70 °C / 170 °C	EVA		Curing Time (h) at 70 °C / 170 °C	ESO	
	1857 cm <sup>-1</sup>	1787 cm <sup>-1</sup>		1857 cm <sup>-1</sup>	1787 cm <sup>-1</sup>
1 / 0	37 ± 3%	34 ± 3%	24 / 0	70 ± 3%	62 ± 3%
2 / 0	48 ± 2%	46 ± 2%	24 / 1	77 ± 2%	66 ± 2%
2 / 1	97 ± 2%	92 ± 2%	24 / 2	79 ± 2%	69 ± 1%
2 / 2	98 ± 1%	95 ± 1%			

## References

1. M. Jabłoński and A. Przepiera, *Journal of Thermal Analysis and Calorimetry*, 2001, **65**, 583-590.
2. A. Khawam and D. R. Flanagan, *The Journal of Physical Chemistry B*, 2006, **110**, 17315-17328.
3. A. Khawam and D. R. Flanagan, *Journal of Pharmaceutical Sciences*, 2006, **95**, 472-498.